# Enhancement of the Dimensional Stability of Poly(ethylene-2,6-naphthalene dicarboxylate) Filament by Multistep Zone Annealing Spinning

HAN GI CHAE,[1] DONG WOOK CHAE,[1] BYOUNG CHUL KIM,[1] SEUNG WON SEO[2]

[1] Division of Chemical Engineering, Hanyang University, 17 Haingdang-Dong, Seongdong-Gu, Seoul 133-791, South Korea

[2] Hyosung Corporation, Anyang 431-080, South Korea

*Received 11 November 2000; accepted 13 February 2001*

**ABSTRACT:** Both good tensile properties and good resistance to thermal shrinkage are prerequisites for tire cord applications. For these purposes, poly(ethylene-2,6-naphthalene dicarboxylate) (PEN) filaments were prepared by multistep zone annealing (MSZA) spinning with a specially devised system. The melting temperature of the PEN filaments so obtained was slightly increased with an increasing total draw ratio. All the filaments exhibited a sharp melting peak around 270°C, but glass-transition behavior was barely visible via differential scanning calorimetry. Rheovibron experiments showed $\alpha$ relaxation in the vicinity of 175°C. Increasing the draw ratio above 4 did not increase the birefringence value much, but it did lead to increases in the tensile properties. The PEN filaments consisted exclusively of $\alpha$-form crystals. The PEN filaments showed excellent resistance to thermal shrinkage, which was less than 1% even with heating to 140°C. In the MSZA spinning process, increasing the degree of hot drawing proved more effective than increasing the degree of cold drawing for obtaining PEN filaments with better dimensional stability at elevated temperatures. © 2002 John Wiley & Sons, Inc. J Appl Polym Sci 83: 916–922, 2002

**Key words:** poly(ethylene-2,6-naphthalene dicarboxylate) (PEN) filament; tire cord; tensile properties; dimensional stability; multistep zone annealing spinning; fiber; thermal properties; crystal structures

## INTRODUCTION

The development of new heavy-duty tire cords has attracted much attention in the automotive industry. Until now, poly(ethylene terephthalate) (PET), nylon, and rayon have been used as materials for tire cords. Tire cords should simultaneously possess high modulus and low shrinkage at elevated temperatures. On this point, PET and nylon have drawbacks because their glass-transition temperatures ($T_g$'s) are not high enough to withstand shrinkage over the service temperatures frequently encountered during high-speed driving. However, high-tenacity rayon has a disadvantage in price.

Poly(ethylene-2,6-naphthalene dicarboxylate) (PEN) is a recently commercialized polyester family that offers a good balance of mechanical and thermal properties. Although PEN fibers have a tenacity similar to that of PET, they give better dimensional stability and lower thermal shrinkage because the naphthalene moiety in PEN in-

*Correspondence to:* B. C. Kim (bckim@hanyang.ac.kr).

Journal of Applied Polymer Science, Vol. 83, 916–922 (2002)

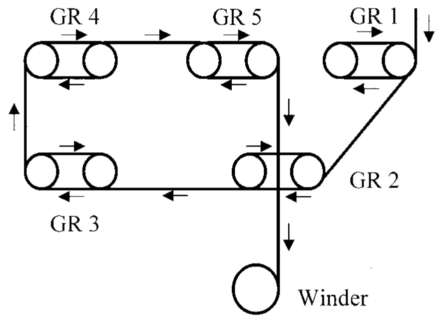


**Figure 1** Schematic description of the MSZA spinning apparatus.

creases stiffness and thermal resistance. PEN has a $T_g$ of about 113°C and melts at 265°C; these temperatures are higher than the $T_g$ and melting temperature ($T_m$) of PET by 38 and 10°C, respectively.[1–10] The high price, however, has limited its commercial applications. Recently, some chemical companies[11–13] succeeded in reducing the price by mass production of the intermediate of the polymer, 2,6-naphthalene dicarboxylic acid.

In this study, various PEN filaments were melt-spun by the adoption of a specially designed multistep zone annealing (MSZA) device, and the effects of drawing and annealing conditions in MSZA spinning on the physical properties of the filaments were investigated.

## EXPERIMENTAL

The PEN filament specimens were prepared by an MSZA spinning unit equipped with specially devised drawing and heating units, the detailed layouts and processing conditions of which are schematically described in Figure 1 and listed in Table I, respectively. The molten PEN was extruded through a spinneret, composed of 204 nozzles, at 322°C. The diameter of the nozzles was 0.4 mm, and the throughput rate was regulated to 275 g/min. The as-spun PEN filaments were drawn by five independent godet rollers (GRs) in series along the spinline. The rotational speeds of the respective rollers were set differently to evaluate the effect of zone annealing conditions on the resultant fiber properties. The draw ratio was determined by division of the rotational speed of a reference roller by that of the first roller. With reference to Table I, the filaments were drawn through GRs 1–4 and relaxed by GR 5. The total draw ratio, the ratio of the rotational speed of the take-up roller to the first GR, was kept constant for all the filament specimens.

The thermal properties were examined via differential scanning calorimetry (DSC) with a DSC-7 (Perkin-Elmer). The first run was performed at a heating rate of 10°C/min for 3–5-mg PEN samples under a dry nitrogen atmosphere. The DSC sample was heated to 300°C. It was held at that temperature for 5 min, and then the molten sample was quenched to 50°C. The same scanning procedure was repeated for the second run.

Dynamic mechanical properties were analyzed with a Rheovibron (Orientec, DDV-01FP). The elastic modulus ($E'$) and loss tangent (tan $\delta$) were measured over a temperature range of 25–275°C. The heating rate was 3°C/min, the dynamic strain was 0.05%, the frequency was 110 Hz, and the hold force was 5 mN/tex.

X-ray beams generated at 40 kV and 100 mA with a rotating-anode X-ray generator (Rotaflex RU-3H, Rigaku-Denki) were monochromatized with a graphite monochromator. The resulting Cu K$\alpha$ X-ray beams were introduced to the specimen through a pinhole collimator 0.5 mm in diameter for wide-angle X-ray diffraction (WAXD). Equato-

**Table I Spinning Conditions for Preparation of PEN Filaments**

| | Rotational Speed (m/min) | | | | | |
|---|---|---|---|---|---|---|
| Roller | GR 1 | GR 2 | GR 3 | GR 4 | GR 5 | Take-Up |
| Roller Temperature | Cold | 130°C | 135°C | 210°C | 110°C | Cold |
| DR 3.0 | 1113 | 1133 | 2700 | 3340 | 3300 | 3310 |
| DR 3.5 | 954 | 974 | 2700 | 3340 | 3300 | 3310 |
| DR.4.0 | 835 | 855 | 2700 | 3340 | 3300 | 3310 |
| DR 4.5 | 742 | 762 | 2700 | 3340 | 3300 | 3310 |
| DR 5.0 | 668 | 688 | 2700 | 3340 | 3300 | 3310 |
| DR 5.5 | 607 | 627 | 2700 | 3340 | 3300 | 3310 |

DR = draw ratio.

rial WAXD measurements were carried out over a $2\theta$ range of 5–40° at a scan speed 5°/min in the reflection mode. To assess the effect of the draw ratio on the microstructure of PEN filaments, we took WAXD photographs in the transmission mode. The camera length of WAXD was 30 mm. All the WAXD patterns were recorded *in vacuo* onto Kodak diagnostic films (DEF5).

Each PEN filament specimen was positioned parallel between microscope glasses and placed at an angle of 45° relative to the crossed polarizers of the microscope, which was equipped with a sodium lamp ($\lambda = 0.5893$ $\mu$m) and a Berek compensator. At the ends of the filaments, which were cut on the bias, the overall difference of phase $\Phi$ was determined by the measurement of the number of fringes (including the partial fringe). For each filament, the birefringence was calculated with the formula $\Delta n = (\Phi/2\pi)(\lambda/D)$, where $D$ is the diameter of the filament. To examine the degree of orientation, we took the birefringence of fully oriented PEN filament as 0.487 for the reference point.[6]

Thermal shrinkage in hot air (120, 140, and 160°C) for 10 min was measured. The initial length of the filaments was about 500 mm, and no tension was applied during measurement. Tensile properties were measured with an Instron tester (model 4465) equipped with standard fiber grips. The gauge length was 20 mm, and the crossover head speed was 10 mm/min. An average value of 10 measurements for each sample was taken as data. The average filament thickness was determined by the weighing of a 1-m bundle composed of 612 filaments. All the samples heat-treated were used as WAXD specimens.

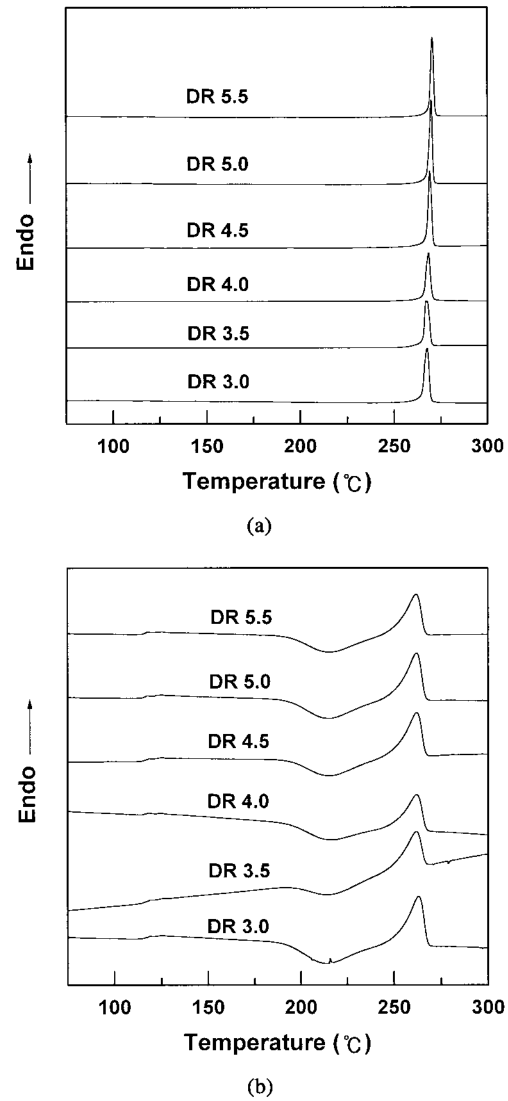


**Figure 2** DSC curves of PEN filaments prepared by MSZA: (a) first and (b) second scan curves.

## RESULTS AND DISCUSSION

For the fiber-spinning process, the stretching ratio in the respective zones is given in Table II. The filament with a higher draw ratio undergoes less cold stretching between the nozzle and GR 1 but is subject to greater hot stretching between GR 1 and GR 3 (the hot draw ratio), and vice versa. Consequently, greater annealing is given to the filament with the higher draw ratio. In all cases, the filament becomes relaxed between GR 4 and GR 5, and only a little tension is exerted on the filament between GR 5 and the take-up roller. The total draw ratio between the nozzle and take-up roller is the same for all the PEN filament specimens.

**Table II Stretching Between GRs**

| | Stretching Ratio Between | | |
|---|---|---|---|
| | Nozzle/GR 1 | GR 1/GR 2 | GR 2/GR 3 |
| DR 3.0 | 139.125 | 1.018 | 2.38 |
| DR 3.5 | 119.25 | 1.021 | 2.77 |
| DR.4.0 | 104.375 | 1.024 | 3.16 |
| DR 4.5 | 92.75 | 1.027 | 3.54 |
| DR 5.0 | 83.5 | 1.03 | 3.92 |
| DR 5.5 | 75.875 | 1.033 | 4.31 |

DR = draw ratio.

Figure 2(a,b) shows DSC thermograms of PEN filaments obtained during the first and second runs, respectively. The analytical values of the DSC results are given in Table III. All the fila-

**Table III DSC Results for the PEN Filaments**

| | | Draw Ratio | | | | | |
|---|---|---|---|---|---|---|---|
| | | 3.0 | 3.5 | 4.0 | 4.5 | 5.0 | 5.5 |
| First run | $T_m$ (°C) | 266.7 | 266.9 | 268.5 | 269.2 | 270 | 270.5 |
| | $\Delta H_m$ (J/g) | 53.966 | 45.913 | 44.851 | 53.822 | 56.742 | 52.727 |
| Second run | $T_m$ (°C) | 262.9 | 261.9 | 262.2 | 262.2 | 262 | 261.9 |
| | $\Delta H_m$ (J/g) | 30.542 | 19.156 | 22.401 | 24.248 | 27.373 | 25.086 |

$\Delta H_m$ = heat of fusion.

ments exhibit a sharp melting peak in a narrow temperature range in the vicinity of 270°C, but the glass-transition behavior is barely observable. With an increasing hot draw ratio, $T_m$ is slightly increased, and the melting peak becomes sharper and the half width of the peak decreases. This suggests that a more perfect and more uniform crystal structure is obtained at a higher hot draw ratio. This is expected because more effective annealing is conferred on the filament at a higher hot draw ratio. In addition, $E'$ and tan $\delta$ of PEN filaments by the Rheovibron are plotted against temperature in Figure 3 to clarify the glass-transition behavior. As the hot draw ratio is increased, $E'$ is increased, the peak temperature of tan $\delta$ corresponding to the $\alpha$ relaxation ($T_g$) is shifted to a higher temperature, and the peak intensity is reduced. This suggests that more molecules in the amorphous region become ordered with increasing orientation. The $\beta$ relaxation is also found in the vicinity of 85°C.

Sometimes, the microstructure of highly oriented filaments can be more clearly revealed by multiscanning of the filament specimens. In this study, the second heating run is obtained for the first-run PEN specimen after it has been fully

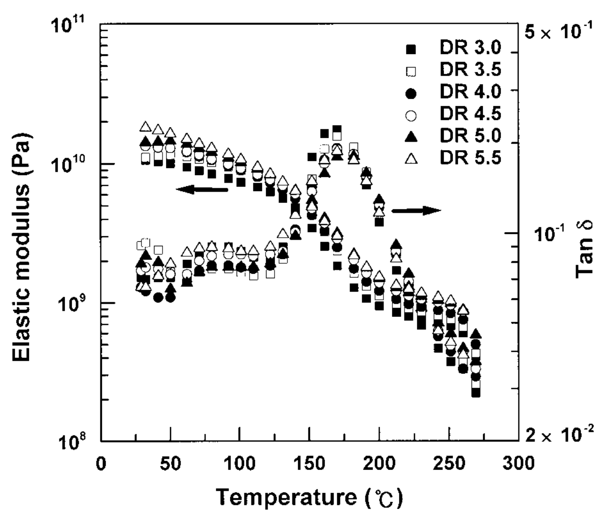


**Figure 3** Variation of the elastic modulus and tan $\delta$ with temperature for PEN filaments prepared by MSZA.

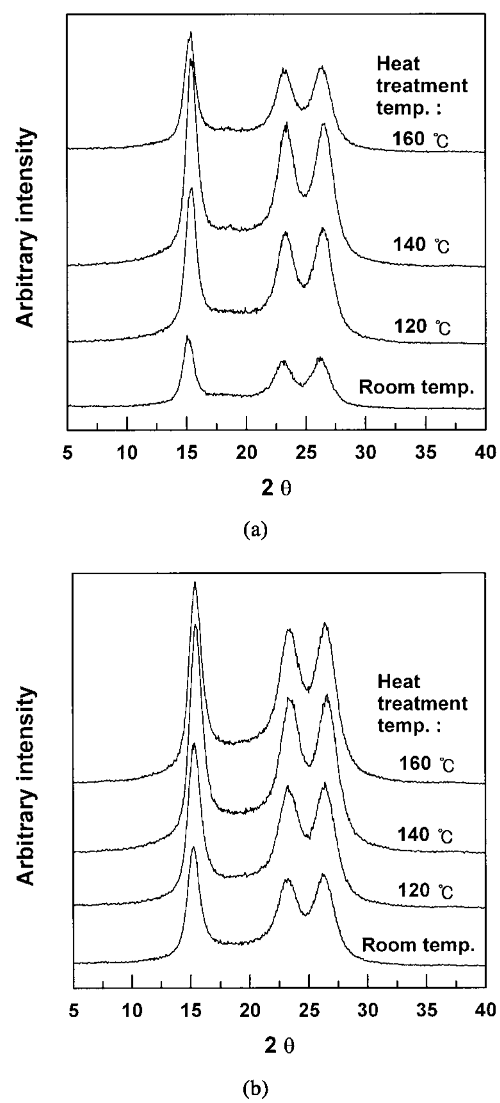


**Figure 4** Equatorial WAXD patterns of PEN filaments prepared by MSZA, showing the effect of the draw ratio (DR) and additional heating on the crystal structures of the filaments: (a) DR = 3.0 and (b) DR = 5.5.

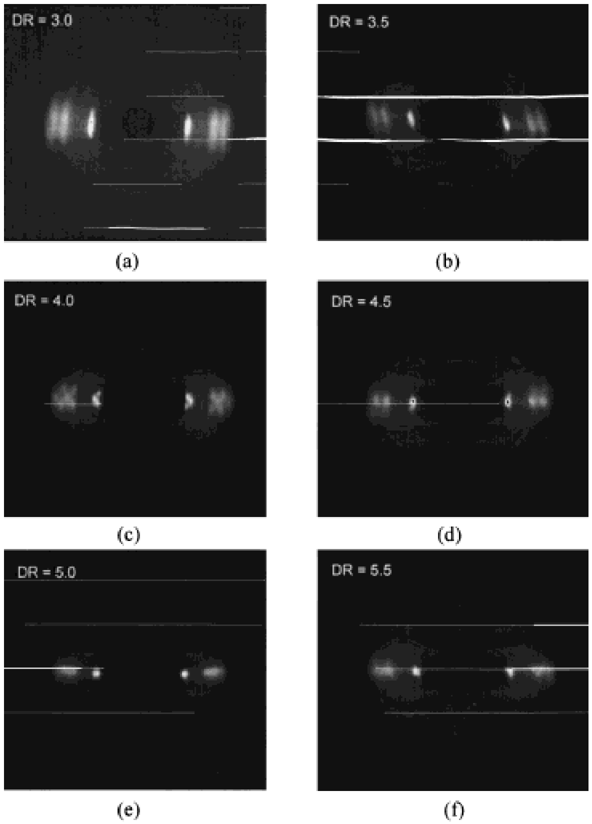


**Figure 5** Photographs of equatorial WAXD patterns by MSZA, showing the effect of the draw ratio (DR) and additional heating on the molecular orientation of the filaments: (a) DR = 3.0, (b) DR = 3.5, (c) DR = 4.0, (d) DR = 4.5, (e) DR = 5.0, and (f) DR = 5.5.

melted at 300°C for 5 min to eliminate remaining structures and residual stresses. The second-run DSC curve so obtained in Figure 2(b) is different from the first curve in Figure 2(a) in two points; the second run exhibits glass-transition behavior, and there is a shift of the melting peak to a lower temperature by about 10°C. On the second heating scan obtained after the cooling of the fully melted PEN specimen to room temperature, glass-transition behavior appears at 120°C. This indicates that much of the amorphous region of PEN is transformed into a mesophase in the filament. In addition, the decrease in $T_m$ in the second run suggests that the crystalline structure of PEN, recrystallized from its melt, is different from that of the PEN filament. The decrease in $T_m$ in the recrystallized specimen indicates that the PEN filament has a more perfect crystalline structure than the recrystallized one. Hence, this thermal analysis verifies that the filaments are mainly composed of two phases, a crystalline phase and a mesophase, in which almost all the molecules in the amorphous region are perfectly ordered by effective annealing in MSZA spinning.

It is reported that PEN produces different forms of crystals, largely depending on the crystallization temperature and drawing. Nagai et al.[14] reported that drawn PEN filaments have a transition of the crystal structure from the $\alpha$ form to the thermodynamically more stable $\beta$ form by tensionless heat treatment. However, cold drawing is known to bring about a transition from the $\beta$ form to the $\alpha$ form.[14] Figure 4 shows equatorial WAXD patterns of the PEN filament specimens. Figure 4 suggests that the crystal of the PEN filament specimen takes the $\alpha$ form. In the figure, the peaks at 15.6, 23.2, and 26.2° are assigned to the (010), (100), and (−110) planes of the crystal, respectively. A small crystalline peak shift with a changing draw ratio was observed even for the heat-treated samples, suggesting that the crystal structure is little affected by drawing at 160°C. This agrees with the previous result[14] that the $\alpha$-form crystal is transformed to the $\beta$-form crystal only when the heat-treatment temperature exceeds 200°C.

To investigate the molecular orientation, we photographed WAXD patterns; they are shown in Figure 5. The off-equator layer lines move to the equator and become concentrated there in the WAXD pattern with an increasing draw ratio. These results indicate that the unoriented amorphous region in the filament becomes ordered with an increasing draw ratio in the MSZA drawing process, and the crystalline phase at a higher

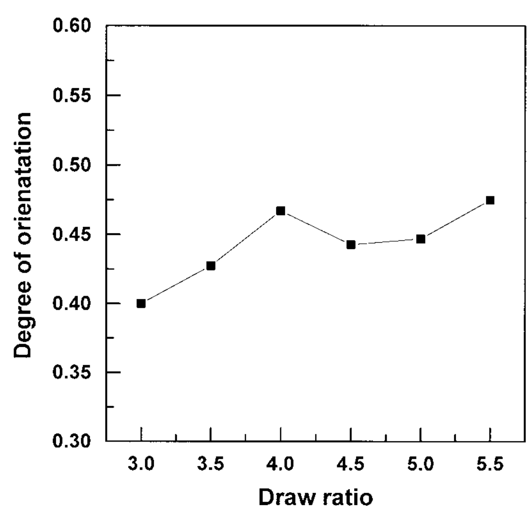


**Figure 6** Variation of the degree of orientation with the draw ratio for PEN filaments by birefringence.

draw ratio becomes a more perfect structure. This agrees with the previous thermal analysis.

Figure 6 presents a plot of the degree of orientation of PEN filaments against the hot draw ratio by birefringence. The PEN filaments obtained by MSZA drawing give an unusually high degree of orientation, 0.48, a value much greater than that reported for most oriented PET filaments, 0.3. The high degree of orientation seems to originate from the high stiffness of the naphthalene ring, which is helpful for the alignment of PEN molecules in the spinline.[15] In addition, the degree of orientation is increased with an increasing hot draw ratio up to a draw ratio of 4. However, a further increase in the hot draw ratio does not produce a notable increase in the degree of orientation in the MSZA spinning process.

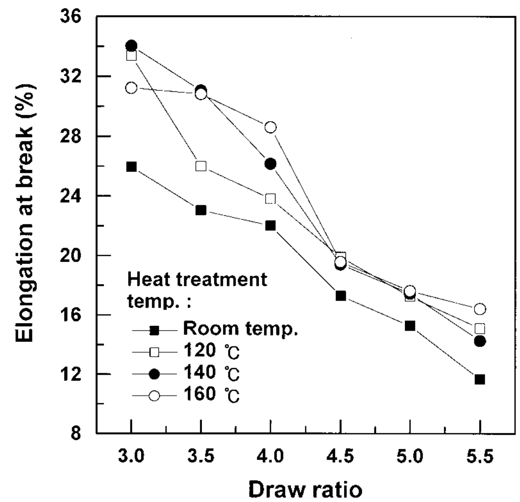


**Figure 8** Variation of the elongation at break with the draw ratio for PEN filaments prepared by MSZA.

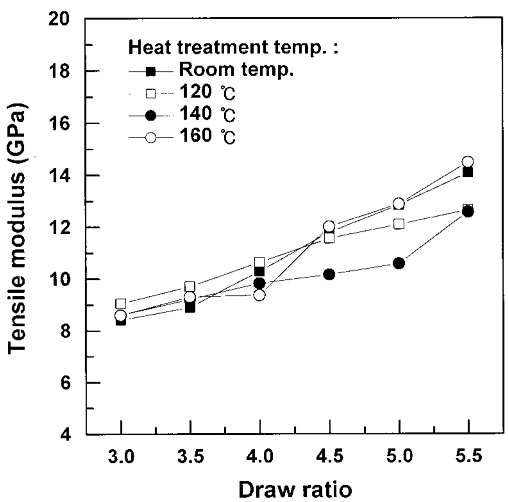


(a)

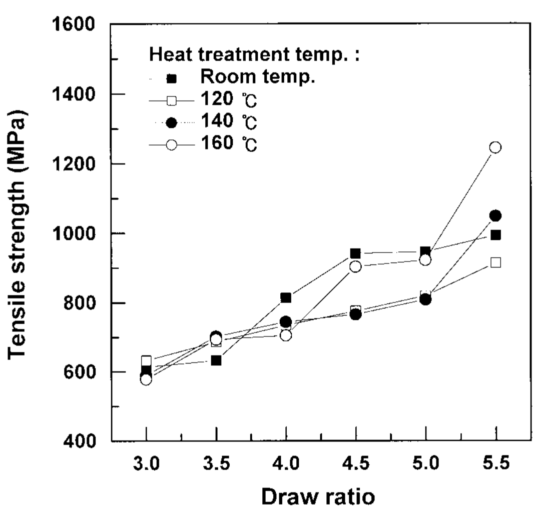


(b)

**Figure 7** Variation of the tensile properties with the draw ratio for PEN filaments prepared by MSZA: (a) tensile modulus and (b) tensile strength.

Tensile properties of PEN filaments are shown in Figure 7. As expected, the tensile modulus and tensile strength are increased with an increasing hot draw ratio. Unlike the results from birefringence and WAXD patterns, the tensile properties of PEN filaments monotonically increase as the hot draw ratio is increased. This seems to result from the increase in molecular orientation, particularly in the amorphous region.

The tensile properties of filaments depend on orientation in the amorphous region and in the crystalline region. However, Figure 7 indicates that little rearrangement of the molecular structure takes place after heat treatment. In other words, the inner structure of PEN filaments is already well established during MSZA spinning. Elongation at break still decreases with a further increasing hot draw ratio higher than 4, as shown in Figure 8. Consequently, increasing the hot drawing is more effective than increasing the cold drawing to acquire more desirable physical properties for tire cord applications.

The shrinkage of PEN filaments at elevated temperatures offers a quantitative measure of dimensional stability, which is a crucial point for tire cords. Figure 9 shows the effect of the hot draw ratio on the thermal shrinkage of PEN filaments at three different temperatures. It is believed that tire cord under extreme conditions should withstand thermal distortion or thermal shrinkage up to 120–130°C. Because of its low $T_g$

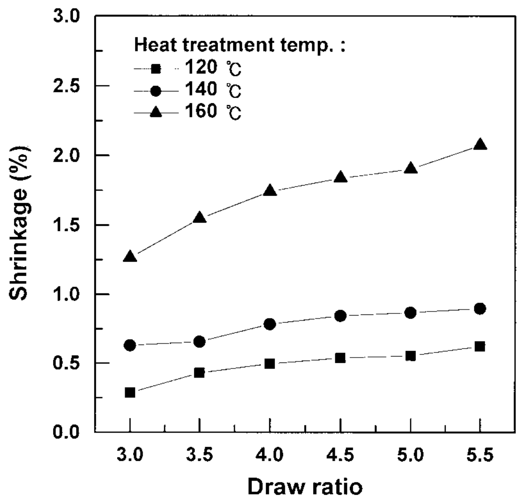


**Figure 9** Variation of the thermal shrinkage with the draw ratio for PEN filaments prepared by MSZA.

(ca. 70°C), PET may cause problems: the highly oriented PET filaments can shrink in the service temperature range that high-speed cars sometimes encounter. When heated to 140°C, the PEN filaments produce less than 1% shrinkage, whereas the PET fibers show greater than 6% shrinkage.[16] The PEN filaments produce only a little shrinkage, even at 160°C.

## CONCLUSION

The MSZA spinning method proved effective and successful in preparing high-performance PEN tire cords with good dimensional stability at elevated temperatures. The MSZA-spun PEN filaments showed glass-transition behavior only with Rheovibron tests and exhibited less than 1% thermal shrinkage even after exposure to 140°C for 10 min. Thus, the MSZA spinning process is recommended for obtained PEN tire cords for severe service conditions.

## REFERENCES


1. Buchner, S.; Wiswe, D.; Zachmann, H. G. Polymer 1989, 30, 480.
2. Cheng, S. Z. D.; Wunderlich, B. Macromolecules 1988, 21, 789.
3. Cheng, S. Z. D.; Wunderlich, B. Thermochim Acta 1988, 134, 161.
4. Ajii, A.; Guevremont, J.; Cole, K. C.; Dumoulin, M. H. Polymer 1996, 37, 3707.
5. Naik, S. G.; Bhat, N. V. Polymer 1986, 27, 333.
6. Jager, J.; Jujin, J. A.; Van Den Heuvel, C. J. M.; Huijts, R. A. J Appl Polym Sci 1995, 57, 1429.
7. Cheng, S. Z. D.; Janimark, J. J.; Zhang, A.; Guan, J.; Chu, A. L. Polym Bull 1988, 20, 449.
8. Ouchi, I.; Aoki, H.; Shimotsuma, S.; Asai, T.; Hosoi, M. Proc Jpn Congr Mater Res 1974, 17, 217.
9. Cakmak, M.; Wang, Y. D.; Simhambhatla, M. Polym Eng Sci 1990, 30, 721.
10. Ito, M.; Honda, K.; Kanamoto, T. J Appl Polym Sci 1992, 46, 1013.
11. Cakmak, M.; Kim, J. C. J Appl Polym Sci 1997, 64, 729.
12. Miyata, K.; Kikutani, T.; Okui, N. J Appl Polym Sci 1997, 65, 1415.
13. Murakami, S.; Nshikawa, Y.; Jsuji, M.; Kawaguchi, A.; Kohija, S.; Cakmak, M. Polymer 1995, 36, 291.
14. Nagai, A.; Murase, Y.; Kuroda, T.; Matsui, M.; Mitsuishi, Y.; Miyamoto, T. Sen-I Gakkaishi 1995, 51, 10.
15. Jackson, W. J. Macromolecules 1983, 16, 1027.
16. Chen, J. Y.; Tucker, P. A.; Cuculo, J. A. J Appl Polym Sci 1997, 66, 13.